Probiotics and Antimicrobial Proteins
https://doi.org/10.1007/s12602-024-10330-3

RESEARCH

Colon Cancer Cells Treated with *Lacticaseibacillus casei* Undergo Apoptosis and Release DAMPs Indicative of Immunogenic Cell Death

Georgios Aindelis[1] · Vassilis Glaros[1,2] · Konstantinos Fragkoulis[1,3] · Areti Mouchtari[1] · Katerina Spyridopoulou[1] · Katerina Chlichlia[1]

Accepted: 17 July 2024

Abstract
Probiotic bacteria, and especially lactic acid bacteria, have long been known to wield a variety of health-beneficial effects, including antioxidant, antimicrobial, anti-inflammatory, immunomodulatory, and anticancer activities. However, our understanding of the mechanisms involved in these activities remains incomplete. In this study, we wished to investigate the processes that give rise to the anticancer activity of *Lacticaseibacillus casei* ATCC393 and the possibility that immunogenic cell death of cancer cells can be induced following treatment with this probiotic. In both cell lines that we have examined, we detected notable pro-apoptotic signaling, including the upregulation of death receptors, that culminated in the activation of caspase 3, the endpoint and most characteristic effector molecule of all pro-apoptotic cascades. In addition, we identified damage-associated molecular patterns associated with immunogenic cell death. Calreticulin exposure on the outer cell membrane, HMGB1 translocation outside the nucleus and depletion of intracellular ATP was evident in both cancer cell lines treated with the probiotic, while expression of type I interferons was upregulated in CT26 cells. Our findings suggest that treatment with the probiotic induced apoptosis in cancer cells, mediated by extrinsic death receptor signaling. Moreover, it resulted in the release of molecular signals related with immunogenic cell death and induction of cancer cell-specific adaptive immune responses.

Keywords Probiotic · *L. casei* · Cancer · Apoptosis · Immunogenic cell death · Calreticulin

Introduction

Probiotics are viable microorganisms that endow the host with health benefits, when consumed in adequate amounts [1]. Lactic acid bacteria (LAB) are an heterogeneous group of Gram-positive bacteria that produce lactic acid as the main end product of carbohydrate metabolism [2]. Their functionality has been shown to include antioxidant [3, 4], antimicrobial [5, 6], anti-inflammatory [7, 8], immunomodulatory [3, 9–11], and anticancer effects [12–14]. However, while several mechanisms have been proposed to delineate the anticancer activity of LAB, a conclusive explanation has not been formed yet.

Among the various functions of LAB, the capability of certain strains to selectively kill cancer cells, specifically by induction of apoptosis, has emerged as a promising alternative, protective measure against malignant disorders [13]. Apoptosis, the de facto modality of regulated cell death, is rigorously controlled by a variety of death receptor/ligand interactions and stress-induced signals, as well as a network of pro- and anti-apoptotic regulatory proteins [15, 16]. Apoptosis realization is characterized by the activation of proteolytic caspases and culminates in morphological and biochemical modifications and eventually cell death [17, 18]. Historically, apoptosis and regulated cell death in general have been considered immunologically tolerogenic and incapable of evoking antigen-specific immunity [19]. However,

✉ Katerina Chlichlia
achlichl@mbg.duth.gr

[1] Department of Molecular Biology and Genetics, School of Health Sciences, Democritus University of Thrace, 68100 Alexandroupolis, Greece

[2] Present Address: Department of Medicine, Division of Immunology and Allergy, Stockholm and Center for Molecular Medicine, Karolinska Institutet, Karolinska University Hospital, Karolinska Institutet, Stockholm, Sweden

[3] Present Address: Department of Microbiology, Tumor and Cell Biology, Karolinska Institute, 171 77 Stockholm, Sweden

Published online: 16 September 2024

more recently, certain types of programmed cell death have been identified as able to induce adaptive immune responses. These cases have collectively been defined as immunogenic cell death [20]. Immunogenicity emerges from the combination of tumor cell antigens and damage-associated molecular patterns (DAMPs), such as calreticulin, high mobility group box 1 (HMGB1) protein, ATP, and type I interferons (IFN) released from dying cancer cells that act as potent immunostimulatory adjuvants [21, 22].

Our goal in this study was to provide a more in-depth examination of the pro-apoptotic activity of *Lacticaseibacillus casei* against the colonic cancer cell lines CT26 and HT29, as well as the possibility that certain immunostimulatory signals could arise from the treated cancer cells, that can then drive forward a more potent antitumor immune response.

Materials and Methods

Materials

Dulbecco's Modified Eagle's Medium (DMEM) was purchased from Gibco (Waltham, MA, USA). Fetal bovine serum (FBS), trypsin, penicillin/streptomycin, and phosphate-buffered saline (PBS) were purchased from Biosera (Boussens, France). MRS Broth, LAB094 was purchased from LabM (Bury, UK). Acetic acid, trichloroacetic acid (TCA), Trizma base, sulforhodamine B (SRB), and all other chemicals mentioned were purchased from Sigma-Aldrich (St. Louis, MO, USA). Antibodies were purchased from Cell Signaling (Danvers, MA, USA), Abcam (Cambridge, UK), Sigma-Aldrich (St. Louis, MO, USA), and Invitrogen (Waltham, MA, USA).

Cell Lines

Mouse CT26 and human HT29 cancer cells were cultured in DMEM medium containing 4.5 g/mL glucose, supplemented with 10% fetal bovine serum (FBS), 2 mM glutamine, penicillin (100 U/mL), and streptomycin (100 μg/mL) and maintained in a humidified atmosphere with 5% CO_2, at 37 °C. Treatments with *L. casei* were done at the same conditions in DMEM with 1 g/mL glucose (low glucose), supplemented as above.

Lacticaseibacillus casei Culture and Preparation

Lacticaseibacillus casei ATCC 393 was cultivated in De Man, Rogosa and Sharpe (MRS) broth at 37 °C without agitation. Bacteria were harvested at the late-log/early stationary phase (10^9 CFU/mL) by centrifugation of the bacterial culture at 1700 × *g*, 4 °C for 15 min and after a washing step with PBS they were re-suspended in low glucose DMEM at the appropriate concentration.

Cell Viability Analysis

The effect of *L. casei* on the viability of cancer cells was evaluated with the SRB assay [23]. Cells were seeded in 96-well plates at a density of 8000 cells (CT26) or 16,000 cells (HT29) and then treated with various concentrations of *L. casei* (10^9–10^6 CFU/mL) for 24, 48, and 72 h. Treated cells were then fixed with 10% TCA and stained with 0.057% w/v SRB. Following extensive washing with 1% v/v acetic acid, protein-bound dye was dissolved in 10 mM Tris base and absorbance at 492 nm was measured with an Enspire multimode plate reader (EnSpire, Perkin Elmer). Viability was estimated in comparison to cancer cells grown only in low glucose DMEM.

Estimation of Gene Expression

Differential gene expression was examined with real-time PCR. Cancer cells were seeded in 60-mm plates at a density of 0.5×10^6 cells (CT26) or 0.8×10^6 cells (HT29) and treated with 10^8 or 10^7 CFU/mL for the indicated time points. Control cells were cultured in DMEM. Following treatment, cells were washed three times with ice cold PBS and then harvested in 1 mL Nucleozol (Macherey–Nagel, Düren, Germany) for RNA isolation. The High-Capacity cDNA Reverse Transcription Kit (Applied Biosystems, Waltham, MA, USA) was employed for cDNA synthesis and real-time PCR was performed in a StepOne™ Real-Time PCR System (Applied Biosystems, Waltham, MA, USA) and using the KAPA SYBR® FAST qPCR Master Mix (2X) Kit (Kapa Biosystems, Wilmington, MA, USA) to prepare the reactions according to supplier's instructions. Beta actin and GAPDH were used as housekeeping genes and expression was calculated with the 2^{-ddCt} method. Primers used are stated in Table 1.

Protein Expression Assessment

Western blot was utilized for the analysis of protein levels after treatment with the probiotic. Cancer cells were seeded in 100-mm plates at a density of 1.5×10^6 cells (CT26) or 2.1×10^6 cells (HT29) and treated with 10^8 or 10^7 CFU/mL for the indicated time points. Control cells were cultured in DMEM. Following treatment, cells were washed three times with ice cold PBS, detached from plates with 7.5 mM PBS-EDTA and collected after centrifugation at 500 × *g*, 4 °C for 5 min. Cells were processed with RIPA buffer (25 mM Tris-Base, 150 mM NaCl, 0.1% w/v SDS, 0.5% w/v sodium deoxycolate, 1% v/v NP40, 1 mM DTT) for the isolation of all cellular proteins or a lysis buffer optimized for the isolation

of cytoplasmic proteins (10 mM HEPES pH 7.9, 10 mM KCl, 0.1 mM EDTA, 1.5 mM $MgCl_2$, 0.2% v/v NP40, 1 mM DTT). In the second case, lysates were incubated at 4 °C for 30 min with occasional vortex and then centrifuged at 1000 × *g*, 4 °C for 10 min. The supernatant containing cytoplasmic proteins was collected and nuclear extracts were prepared by resuspending the pellet in lysis buffer and sonication. All lysis buffers were supplemented with protease (PMSF 100 μg/mL, Leupeptin 0.5 μg/mL, Aprotonin 0.5 μg/mL, Pepstatin 1 μg/mL) inhibitors and phosphatase (1 mM β-glycerophosphate, 1 mM Na_3VO_4) inhibitors. Protein concentration was quantified with the BCA assay, utilizing a BSA standard curve. Equal amounts of proteins were subjected to SDS-PAGE in 8%, 10%, or 12% Tris–glycine gels and then transferred onto PVDF membrane (Merck Millipore, Burlington, MA, USA). Blocking of non-specific binding was achieved by incubating membranes for 2 h at room temperature (RT) in 5% non-fat dry milk in 150 mM NaCl, 100 mM Tris pH 7.5, 0.1% (v/v) Tween-20. Primary antibodies (survivin 2808, Cell Signaling 1:1000; caspase 3 9662, Cell Signaling 1:1000; cleaved caspase 3 9661, Cell Signaling 1:500; human cleaved PARP1 9541, Cell Signaling 1:1000; mouse cleaved PARP1 9544, Cell Signaling 1:1000; Puma 12450, Cell Signaling 1:1000; Bax 5023, Cell Signaling 1:1000; lamin B2 13823, Cell Signaling 1:1000; HMGB1 ab18256, Abcam 1:1000; b-tubulin T7816, Sigma Aldrich 1:20000) were incubated overnight at 4 °C with gentle shaking and then with anti-rabbit (7074, Cell Signaling 1:2000) or anti-mouse (7076, Cell Signaling 1:2000) HRP-conjugated antibodies. Signal visualization was performed with ECL chemiluminescent substrate and exposure in films.

Detection of Caspase 3 Activation, HMGB1 Translocation, Calreticulin exposure, and ATP Exhaustion by Fluorescence Microscopy

Cancer cells were seeded onto glass coverslips and then treated with 10^8 or 10^7 CFU/mL for the indicated time points. Control cells were cultured in DMEM. Following treatment, cells were washed three times with ice cold PBS and fixed with 4% PFA for 10 min. For the detection of HMGB1 and cleaved caspase 3, fixed cells were permeabilized with 0.2% Triton X-100, while there was not a permeabilization step in cells intended for the detection of calreticulin translocation. Coverslips were then blocked with 2% FBS and stained with primary antibodies (cleaved caspase 3 9661, Cell Signaling 1:200; HMGB1 ab18256, Abcam 1:500; calreticulin ab2907, Abcam 1:500) for 1 h at RT, followed by 3 washes and incubation for 30 min with an Alexa Fluor-488-conjugated anti-rabbit antibody (A11008, Invitrogen 1:1000). Nuclei were stained with 200 ng/mL Hoechst 33342 for 15 min; coverslips were washed a final three times and mounted onto glass slides. ATP-containing vesicles were detected in live cells seeded onto coverslips. Following treatment with the probiotic, cancer cells were washed 3 times and then stained with 4 μM quinacrine and 200 ng/mL Hoechst 33342 for 20 min at RT and then thoroughly washed with PBS. All samples were imaged with a Zeiss Axio Scope A1 microscope and ZEN Blue imaging software by Carl Zeiss Microscopy (Jena, Germany). Quantification of HMGB1 and ATP-containing vesicles was performed in ImageJ (1.50i, NIH) according to an established method [24]. In summary, the nucleus outline in the case of HMGB1 and the cellular outline in the case of ATP were drawn, as well as adjacent cell-free areas as background signal. Area, integrated density and mean background fluorescence were quantified and the corrected total cell fluorescence (CTCF) was computed with the formula:

$$\text{CTCF} = \text{integrated density} - (\text{area of selected cell} * \text{mean fluorescence of background readings})$$

Calculated CTCF values of *L. casei*-treated cells were normalized to CTCF values of control cells and expressed as percentage of relative fluorescent intensity.

Evaluation of Apoptosis-Related Proteins with Membrane- and Glass-Based Sandwich Immunoassays

Commercially available kits were used for the evaluation of protein levels of apoptosis-related proteins in CT26 (ARY031, R&D Systems, Minneapolis, MI, USA) and HT29 (12856, Cell Signaling, Danvers, MA, USA) cells. Cancer cells were seeded in 100-mm plates at a density of 1.5×10^6 cells (CT26) or 2.1×10^6 cells (HT29) and treated with 10^8 CFU/mL for 27 h and 24 h, respectively. Control cells were cultured in DMEM. Following treatment, cells were washed three times with ice cold PBS, detached from plates with 7.5 mM PBS-EDTA and collected after centrifugation at 500 × *g*, 4 °C for 5 min. Next, 0.5 mL lysis buffer provided by the kit, supplemented with protease and phosphatase inhibitors as mentioned, was added to the cell

pellet and incubated for 30 min at 4 °C with occasional mixing. The lysate was then centrifuged at 14,000 × *g*, at 4 °C for 5 min, and the supernatant was collected. Protein concentration was quantified with the BCA assay and equal amounts of protein were loaded onto each membrane or slide. The rest of both assays was conducted according to manufacturer's protocol. Detection was performed with ECL chemiluminescent substrate with a ChemiDoc MP System (Bio-Rad, Hercules, CA, USA) and signal intensity was calculated with the Protein Array Analyzer plugin in ImageJ.

Analysis of Calreticulin Surface Exposure with Flow Cytometry

Cancer cells were seeded in 35-mm plates at a density of 0.25×10^6 cells (CT26) or 0.35×10^6 cells (HT29) and treated with 10^8 or 10^7 CFU/mL for the indicated time points. Control cells were cultured in DMEM. Following treatment, cells were washed three times with ice cold PBS, detached from plates with 7.5 mM PBS-EDTA and collected after centrifugation at 500 × *g*, 4 °C for 5 min. Cells were incubated with an antibody against calreticulin (ab2907, Abcam 1:500) for 45 min at 4 °C, followed by two washes with FACS buffer (PBS, 2.5% FBS, 2.5 mM EDTA) and staining with an Alexa Fluor488-conjugated anti-rabbit antibody (A11008, Invitrogen 1:1000) for 40 min at 4 °C. Unbound antibody was washed twice with FACS buffer, cells were suspended in 100 µL PBS, and 5 µL 7-aminoactinomycin D (7-AAD, 559925, BD Biosciences, Franklin Lakes, NJ, USA) were added for 5 min. Samples were analyzed in an Attune NxT flow cytometer (Thermo Fisher Scientific, Waltham, MA, USA) and cells positive for 7-AAD (dead) were excluded. Flowing Software 2 (Turku, Finland) was used for data analysis.

Investigation of Caspase Activity

A commercially available fluorescence-based kit (ab219915, Abcam, Cambridge, UK) was employed for the analysis of caspases enzymatic activity, following treatment with *L. casei*. Cells were seeded in a black frame 96-well plate at a density of 8000 cells (CT26) or 16,000 cells (HT29) and then treated with 10^8 or 10^7 CFU/mL for the indicated time points. Control cells were cultured in DMEM. Caspase activity was evaluated using caspase-specific substrates coupled with a fluorophore that is released and emits fluorescence at 450 nm, 525 nm, and 620 nm upon cleavage from caspase 9, caspase 8, or caspase 3, respectively. Substrates were added directly on each well and incubated at RT for 1 h, and then, fluorescence was measured with an Enspire plate reader (PerkinElmer, Waltham, MA, USA). Fluorescence of treatment samples was normalized with values from control, untreated cells.

Statistical Analysis

All data used in statistical evaluation are representative of at least three independent experiments. SigmaPlot version 11 (Systat Software, San Jose CA, USA) was used for the statistical analysis. Cell viability was assessed using ANOVA with post hoc Dunnet's test. Real-time PCR data were analyzed using one sample *t*-test, followed by false discovery rate (fdr) multiple comparison correction. Caspase activity data were analyzed with Student's *t*-test followed by fdr multiple comparison correction. Fluoresce intensity was tested using Wilcoxon's rank sum test. Results were considered significant when $p < 0.05$ ($*p < 0.05$, $**p < 0.01$, $***p < 0.001$).

Results

Lacticaseibacillus casei Suppresses Proliferation of Tumor Cells

The anti-proliferative activity of the probiotic *Lacticaseibacillus casei* against colon cancer cells of human and murine origin was evaluated with the SRB assay. As shown in Fig. 1, there was a significant suppression of cell growth as early as 24 h after treatment, with an approximately 40% reduction in the viability of cancer cells from both cell lines incubated with 10^9 and 10^8 CFU/mL. Treatment with 10^7 CFU/mL of *L. casei* was effectual only after 48 h, and even then, the effect was not very severe, as the decrease in cell growth was only about 20% and peaking at roughly 40% after 72 h.

Lacticaseibacillus casei Induces Apoptotic Cell Death in Murine and Human Colon Cancer Cells

In order to better understand the mechanisms instigating the aforementioned anti-proliferative effect of the probiotic, and taking into account previous observation of our research group [12], we decided to investigate the expression of genes involved in apoptosis regulation. Intriguingly, death receptor genes were those that were found to be more potently upregulated. Expression of the Fas (CD95) gene was significantly increased in both cell lines, in response to treatment with *L. casei* and as early as 6 h post treatment with 10^8 CFU/mL in the case of CT26 cells. In addition, death receptor 4 (DR4) and DR5 expression was amplified in HT29 and CT26 cells, respectively (Figs. 2A, 3A). Interestingly, in CT26 cells Fas (CD95) upregulation was observed prior to that of DR5 and was more prominent, while in HT29 cells it was the other way around. As far as signaling proteins are concerned, gene expression of the pro-apoptotic Bax protein

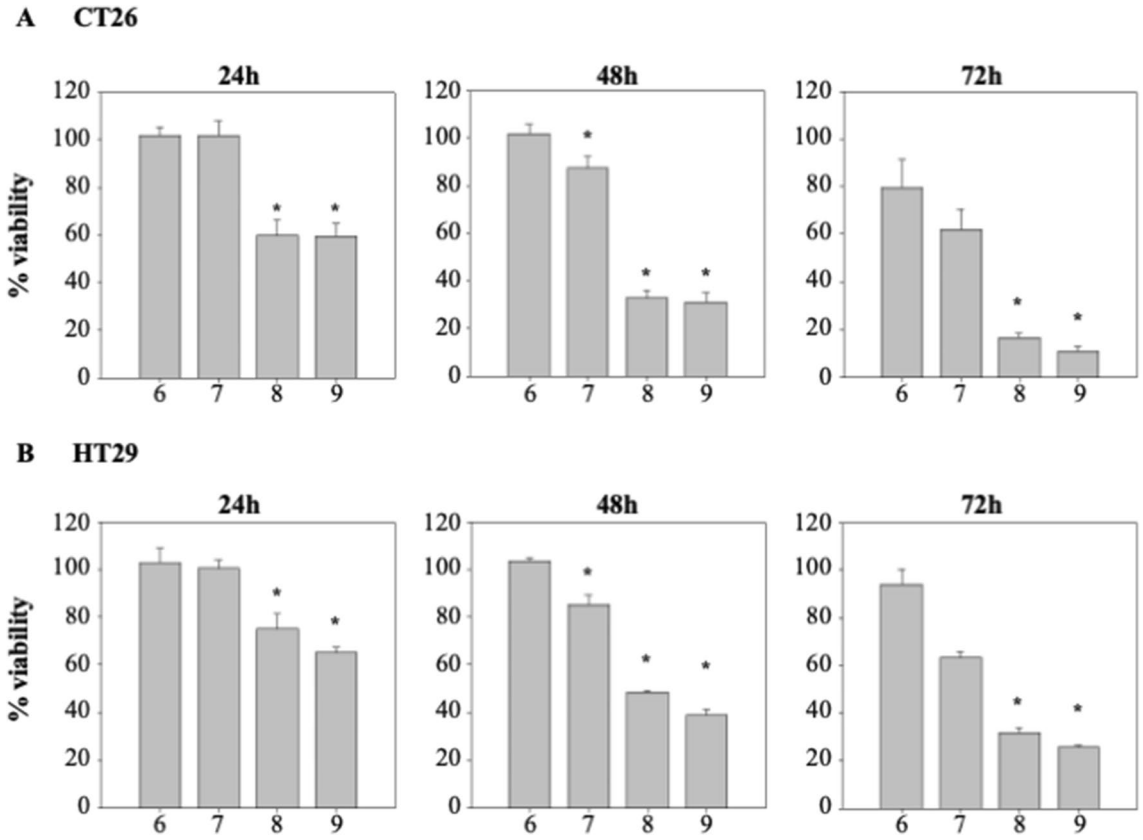

Fig. 1 Suppression of cancer cell proliferation following treatment with *L. casei*. The anti-proliferative effect of *L. casei* on colon cancer cells was evaluated with the SRB assay. CT26 (**A**) and HT29 (**B**) cells were treated with $10^6 - 10.^9$ CFU/mL of *L. casei* for 24 h, 48 h, and 72 h. Viability was calculated as the percentage of cell growth in comparison to cells treated with DMEM. *Lacticaseibacillus casei* concentration is expressed as log CFU/mL. Data shown are mean values ± SD, are representative of at least three independent experiments and were analyzed in SigmaPlot using ANOVA with post hoc Dunnet's test. $^*p < 0.05$

was also increased in both cell lines, while the anti-apoptotic Bcl2 gene was downregulated in CT26 cells and earlier timepoints only. Finally, gene expression of the adaptor FAS-associated death domain (FADD) protein was enhanced in HT29 cells and expression of apoptotic protease-activating factor 1 (APAF-1), a protein involved in the formation of the apoptosome was increased in CT26 cells (Figs. 2A and 3A).

Next, we examined the levels of specific apoptosis-associated proteins, following incubation of cancer cells with *L. casei*. Unsurprisingly, considering the overall complexity of cell proliferation and apoptosis signaling, both anti- and pro-apoptotic modifications were detected. As shown in Fig. 2B, Fas (CD95) and DR5 upregulation was confirmed at the protein level, in accordance to the observations about gene expression. Furthermore, catalase and cytochrome c were detected in increased quantities in probiotic-treated CT26 cells, while claspin levels were notably lower in the same population. More importantly, we observed a distinct accumulation of cleaved caspase 3 in treated cells (Fig. 2B). Similarly, in HT29 cells (Fig. 3B), levels of the anti-apoptotic protein survivin were distinctly lower in *L. casei*-treated cells, as was the phosphorylation of heat shock protein 27 (HSP27) and Akt. On the other hand, phosphorylation of kinases checkpoint kinase 2 (Chk2) and p38 was elevated. As before, cleavage of caspase 3 was found to be increased after treatment with the probiotic and we also detected cleavage of PARP1, a characteristic apoptotic marker (Fig. 3B). In order to confirm our observations on specific, key elements of the apoptotic machinery, we employed western blot analysis. As shown in Figs. 2C and 3C, decreased levels of survivin were detected in CT26 and HT29 cells respectively, as were elevated levels of Bax and Puma in HT29 cells only (Fig. 3C). Finally, we detected an increase of the cleaved, active fragment of caspase 3 in both cancer cell lines using western blot and immunofluorescent microscopy, with a subsequent decrease of the intact procaspase 3 molecule (Fig. 2C–D, Fig. 3D). Considering the aforementioned results, we then decided to evaluate the enzymatic activity of the major initiator and executioner caspases. As depicted in Figs. 2E and 3E, in both CT26 and HT29 cells, caspase 8 was the first to be activated as early as 6 and 12 h following the treatment with probiotics respectively, while

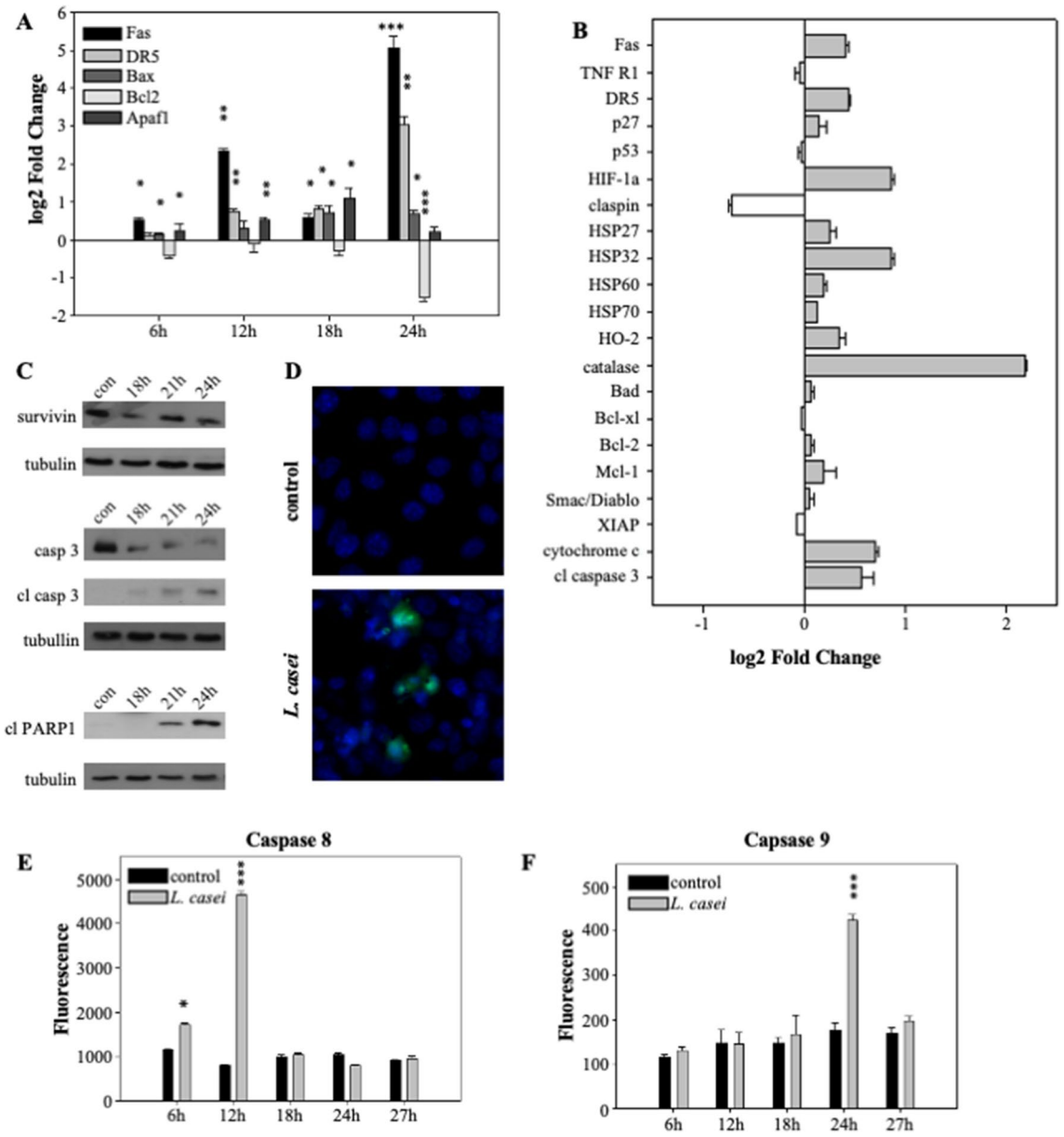

Fig. 2 Treatment with *L. casei* induces apoptosis in CT26 colon cancer cells. CT26 cells were incubated with 10^8 CFU/mL *L. casei* for up to 27 h. **A** Relative gene expression of CT26 cells treated for 6 h, 12 h, 18 h, and 24 h, was estimated with rt-PCR using the 2^{-ddCt} method. Expression was normalized with control cells and presented as $\log_2$Fold change. Bars present mean values ± SD of four independent experiments. **B** Evaluation of apoptosis-related proteins using a commercially available kit (ARY031, R&D Systems), expressed as $\log_2$Fold change in relation to control cells. Gray bars denote upregulation and white ones downregulation. **C** Western blot analysis of survivin, caspase 3, cleaved caspase 3, and PARP1 in *L. casei*-treated CT26 cells for 18 h, 21 h, and 24 h. B-tubulin was used as a loading control. **D** Confirmation of caspase 3 cleavage in CT26 cells. Cancer cells were seeded onto glass coverslips, treated with $10.^8$ CFU/mL *L. casei* for 24 h and stained with an anti-cleaved caspase 3 antibody and a corresponding anti-rabbit AlexaFluor488 conjugated antibody. Images were taken with a fluorescent microscope at 40× magnification. **E**, **F** Caspase 8 and caspase 9 activities in CT26 cells treated for 6 h, 12 h, 18 h, 24 h, and 27 h was assessed with a fluorescence-based kit (ab219915, Abcam). Fluorescence is presented in arbitrary units and bars present mean values ± SD. Control cells were cultured in DMEM. All images excluding apoptosis-related proteins in **B** are representative of at least two independent experiments. Statistical analysis was performed in SigmaPlot, using one sample *t*-test for rt-PCR and Student's *t*-test for caspase activity, followed by fdr multiple comparison correction. $*p < 0.05$, $**p < 0.01$, $***p < 0.001$

caspase 9 (Fig. 2F, Fig. 3F) activation was found to be lagging behind and only being evident after 24 h of culture. One notable difference between the two cell lines was the fact that the activity of caspase 8 in HT29 continued to increase throughout the time course that was inspected, whereas, in CT26 cells, it peaked at 12 h of treatment after which time

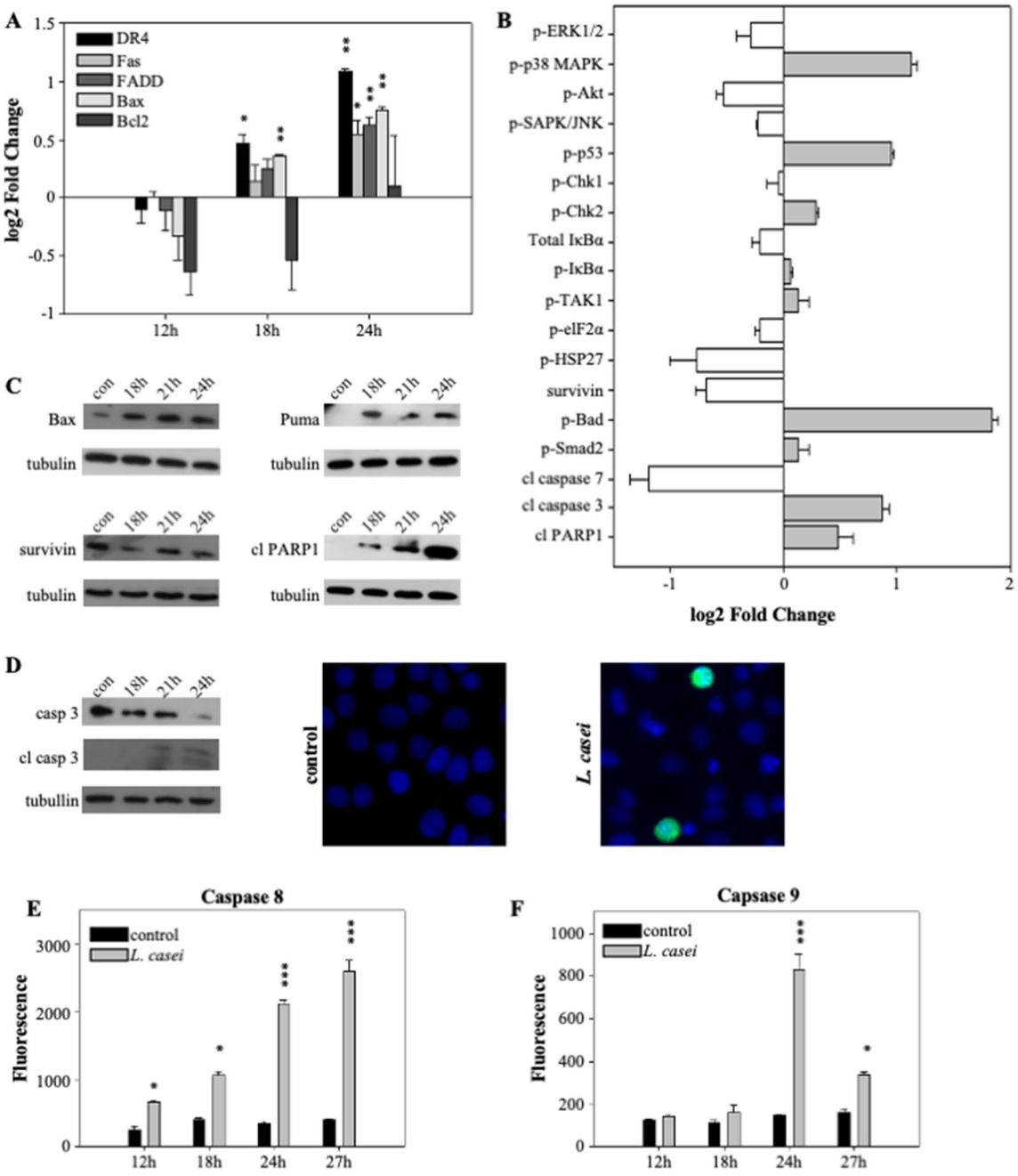

Fig. 3 Human HT29 cells treated with *L. casei* die through apoptotic mechanisms. HT29 cells were incubated with 10^8 CFU/mL *L. casei* for up to 27 h. **A** Relative gene expression of HT29 cells treated for 12 h, 18 h, and 24 h, was estimated with rt-PCR using the 2^{-ddCt} method. Expression was normalized with control cells and presented as $\log_2$Fold change. Bars present mean values ± SD of four independent experiments. **B** Evaluation of cell stress and apoptosis signaling using a commercially available kit (12856 s, Cell Signaling), expressed as $\log_2$Fold change in relation to control cells. Gray bars denote upregulation and white ones downregulation. **C** Western blot analysis of Bax, Puma, survivin, and PARP1 in *L. casei*-treated HT29 cells for 18 h, 21 h, and 24 h. B-tubulin was used as a loading control. **D** Confirmation of caspase 3 cleavage in HT29 cells using Western blot and immunofluorescence. For immunofluorescence, cancer cells were seeded onto glass coverslips, treated with $10.^8$ CFU/mL *L. casei* for 24 h and stained with an anti-cleaved caspase 3 antibody and a corresponding anti-rabbit AlexaFluor488-conjugated antibody. Images were taken with a fluorescent microscope at 40× magnification. **E**, **F** Caspase 8 and caspase 9 activities in HT29 cells treated for 12 h, 18 h, 24 h, and 27 h were assessed with a fluorescence-based kit (ab219915, Abcam). Fluorescence is presented in arbitrary units and bars present mean values ± SD. Control cells were cultured in DMEM. All images excluding cell stress signaling and apoptosis-related proteins in **B** are representative of at least two independent experiments. Statistical analysis was performed in SigmaPlot, using one sample *t*-test for rt-PCR and Student's *t*-test for caspase activity, followed by fdr multiple comparison correction. $*p < 0.05$, $**p < 0.01$, $***p < 0.001$

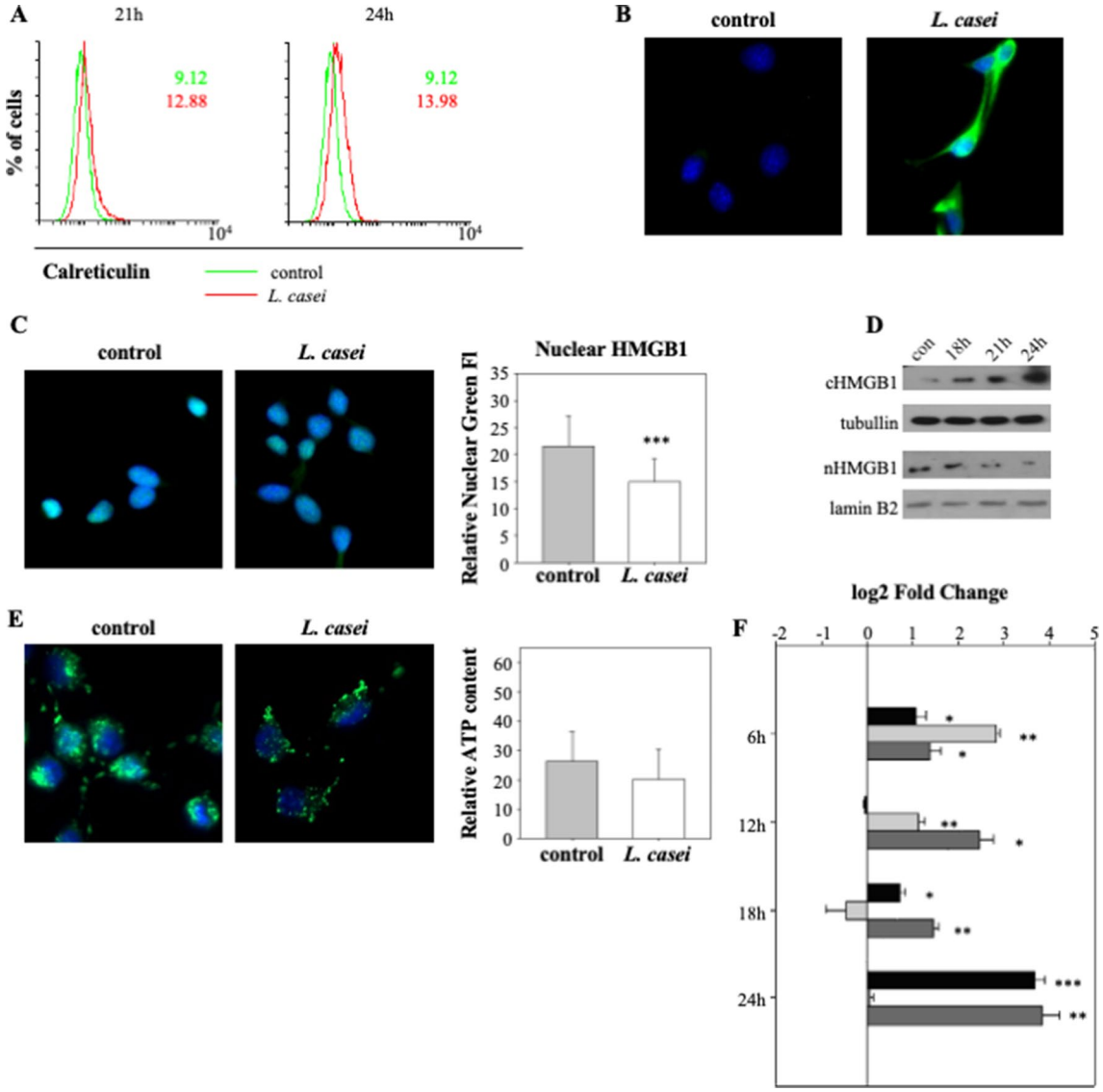

Fig. 4 CT26 cells treated with *L. casei* demonstrate characteristic markers of immunogenic cell death. **A** Calreticulin exposure on the cell membrane was evaluated with flow cytometry. Cancer cells were treated with 10^8 CFU/mL *L. casei* for 21 h and 24 h and then labeled with anti-calreticulin antibody followed by anti-rabbit AlexaFluor488-conjugated antibody. Dead cells were excluded based on staining with 7-AAD and the analysis of calreticulin exposure was restricted on live, 7-AAD-negative scells. Results are presented as fluorescent intensity histograms. **B** Calreticulin exposure was confirmed with fluorescent microscopy. Cells were seeded onto glass coverslips, treated with 10^8 CFU/mL *L. casei* for 24 h and stained with an anti-calreticulin antibody and a corresponding anti-rabbit AlexaFluor488-conjugated antibody. Images were taken with a fluorescent microscope at 40× magnification. **C** Translocation of HMGB-1 out of the nucleus was analyzed with fluorescent microscopy. Cells were treated as above and stained with an anti-HMGB-1 antibody. Quantification of relative nuclear green fluorescence was calculated with ImageJ. Bars present mean values ± SD. **D** HMGB-1 translocation was confirmed with Western blot of cytoplasmic and nuclear protein content of *L. casei*-treated CT26 cells for 18 h, 21 h, and 24 h. B-tubulin and lamin B2 were used as loading controls. **E** The reduction in ATP content of CT26 cells cultured with 10^8 CFU/mL *L. casei* for 24 h was investigated with fluorescent microscopy. Cells were treated as above and stained with quinacrine. Quantification of relative ATP content was measured with ImageJ. Bars correspond to mean values ± SD. **F** Relative gene expression of IFNa2, IFNb, and IL-1β of CT26 cells treated for 6 h, 12 h, 18 h, and 24 h, was estimated with rt-PCR using the $2.^{-ddCt}$ method. Expression was normalized with control cells and presented as $\log_2$Fold change. Bars present mean values ± SD of four independent experiments. Control cells were cultured in DMEM. All images are representative of at least two independent experiments. Statistical analysis was performed in SigmaPlot, using one sample *t*-test, followed by fdr multiple comparison correction for rt-PCR and Wilcoxon's rank sum test for fluorescence analysis. $*p < 0.05$, $**p < 0.01$, $***p < 0.001$

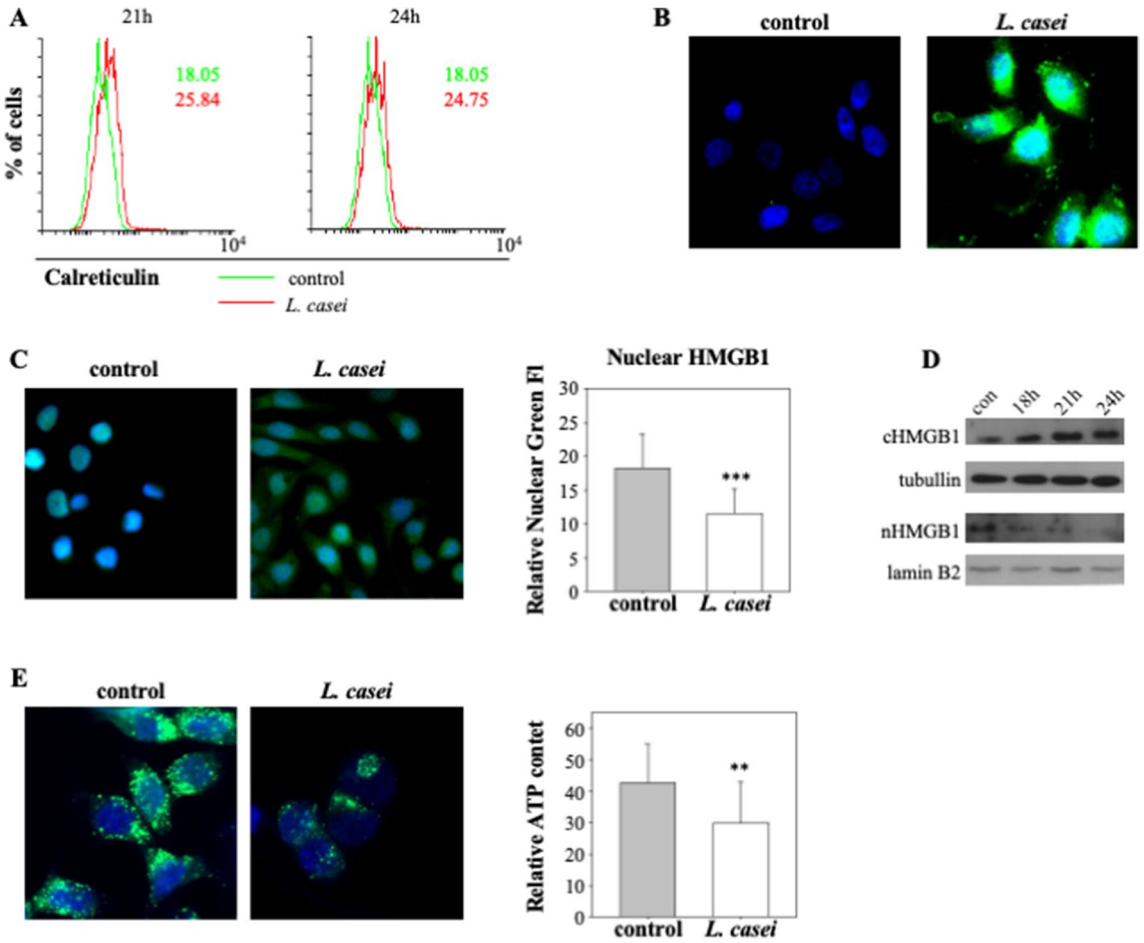

Fig. 5 Treatment of HT29 cells with *L. casei* induced DAMPs release associated with immunogenic cell death. **A** Calreticulin exposure on the cytoplasmic membrane was investigated with flow cytometry. Cancer cells were treated with 10^8 CFU/mL *L. casei* for 21 h and 24 h and then stained with anti-calreticulin antibody followed by anti-rabbit AlexaFluor488-conjugated antibody. Dead cells were excluded based on staining with 7-AAD and the analysis of calreticulin exposure was restricted on live, 7-AAD-negative cells. Results are presented as fluorescent intensity histograms. **B** Calreticulin exposure was evaluated with fluorescent microscopy. Cells were seeded onto glass coverslips, treated with 10^8 CFU/mL *L. casei* for 24 h and labeled with an anti-calreticulin antibody and anti-rabbit AlexaFluor488-conjugated antibody. Images were acquired with a fluorescent microscope at 40× magnification. **C** Localization of HMGB-1 in the nucleus and the cytoplasm was assessed with fluorescent microscopy. Cells were treated as above and stained with an anti-HMGB-1 antibody. Quantification of relative nuclear green fluorescence was calculated with ImageJ. Bars present mean values ± SD. **D** HMGB-1 translocation was investigated with Western blot of cytoplasmic and nuclear protein content of *L. casei*-treated HT29 cells for 18 h, 21 h, and 24 h. B-tubulin and lamin B2 were used as loading controls. **E** The decrease in ATP content of HT29 cells cultured with 10^8 CFU/mL *L. casei* for 24 h was evaluated with fluorescent microscopy. Cells were treated as above and stained with quinacrine. Quantification of relative ATP content was calculated with ImageJ. Bars shown are mean values ± SD. Control cells were grown in DMEM. All images are representative of at least two independent experiments. Statistical analysis was performed in SigmaPlot, using Wilcoxon's rank sum test. $^{**}p < 0.01$, $^{***}p < 0.001$

it subsided down to similar levels to untreated cells. Finally, Western blot was also used in order to verify the cleavage of PARP1 in CT26 (Fig. 2C) and HT29 (Fig. 3C) cells, following treatment with *L. casei*.

The next objective of our research was to examine whether incubation of tumor cells with *L. casei* could elicit immunogenic cell death, a class of programmed cell death distinguished by its ability to promote adaptive immune responses. Crucial role in this phenomenon play DAMPs released from dying cells. To this end, we firstly inspected the exposure of calreticulin, using flow cytometry. As shown in Fig. 4A and Fig. 5A, we detected the presence of calreticulin on the outer layer of the cytoplasmic membrane in both CT26 and HT29 cells treated with the probiotic microorganism. Notably, maximum exposure was observed in different time points in the two cell lines, with CT26 cells displaying maximum calreticulin at 24 h of treatment and HT29 at 21 h. In order to confirm these observations, we utilized fluorescent microscopy and we once again detected calreticulin molecules on the outer

layer of both human and murine tumor cells (Figs. 4B and 5B).

The second DAMP that we decided to investigate was HMGB1. Translocation of this nuclear protein outside of the nucleus and subsequent release into the environment is one of the hallmarks of immunogenic cell death [19]. Once again, both cell lines treated with *L. casei* were found to have a decreased nuclear content of HMGB1 when inspected with fluorescent microscopy (Figs. 4C and 5C). Assessment of both nuclear and cytosolic content of HMGB1 in tumor cells with Western blot supported the fluorescent microscopy results and also revealed that the translocation of HMGB1 out of the nucleus is a time-dependent phenomenon increasing at longer incubations (Figs. 4D and 5D). We then evaluated the release of ATP from treated cancer cells, another DAMP associated with immunogenic cell death. ATP-containing vesicles were stained and visualized with a fluorescent microscope and we noted that the amount of ATP decreased when cells were co-cultured with *L. casei*, with the effect after 24 h being more prominent in HT29 cells (Figs. 4E and 5E). Finally, the last ICD-related signal that we evaluated was the expression of immunostimulatory cytokines, like type I IFN and IL-1β. Surprisingly, here was the first time that we observed a major deviation between the two cancer cell lines that we inspected. While both IFNa2 and IFNβ, as well as IL-1β expression was upregulated at various time points, in probiotic-treated CT26 cell (Fig. 5F), no such increase in the expression of the same genes was detected in HT29 cells (data not shown).

Discussion

Lactic acid bacteria and in particular lactobacilli have long been investigated in relation to their health-promoting properties [1, 2].

As we have previously shown, *Lacticaseibacillus casei* ATCC 393 exerts anti-proliferative effects and induces apoptosis in colon cancer cells, while simultaneously improving antitumor immune effects in a colorectal cancer preclinical model and can also be used as platform for the biosynthesis of selenium nanoparticles with anticancer and immunomodulatory properties [9, 12, 24, 25]. In this study, we aspired to examine in more detail the underlying mechanisms of the pro-apoptotic activity of the probiotic and to investigate its potential as a microbial agent that promotes immunogenic cell death. Our first interesting observation was the upregulation of death receptors in both cell lines, following treatment with the probiotic. Among them, DR4 and DR5 were increased in HT29 and CT26 cells respectively, while Fas (CD95) was elevated in both cell lines. Nevertheless, all of these receptors are initiative components of the extrinsic apoptotic pathway, a cascade of events that culminates in the death of the affected cell [15]. The progression of the pathway hinges on the recruitment of FADD and procaspase 8, the formation of a death-inducing signaling complex (DISC) and ultimately the activation of caspase 8 [26]. Intriguingly, FADD expression was also enhanced in our experiments, which, in combination with previous results of our team indicating the up-regulation of TRAIL [12], a ligand of both DR4 and DR5 [27], led us to hypothesize that the pro-apoptotic activity of *L. casei* was driven through death receptor signaling. As we continued our exploration of apoptotic signaling, we unveiled a significant accumulation of Bax in both cancer cell lines, an important pro-apoptotic protein that interacts with Bcl-2 family members, nullifying them and promoting mitochondrial outer membrane permeabilization (MOMP) [15, 17]. Disruption of the mitochondrial membrane results in the release of cytochrome c from the mitochondria to the cytosol where it binds APAF-1, facilitating oligomerization of individual APAF-1-cytochrome c units into the apoptosome and the activation of caspase 9 [17, 28]. Both cytochrome c and APAF-1 upregulation were evident in CT26 cells treated with *L. casei*. An additional apoptosis-associated protein that was found to be reduced in both cancer cell lines inspected was survivin. Survivin is a multi-role regulator of cell proliferation and apoptosis inhibitor and an example of a distinctly differentially expressed protein in healthy and malignant cells. It acts on various stages of the apoptotic machinery, inhibiting many members of the signaling cascade that concludes in cell death [29, 30].

In addition, examination of various signaling factors involved in cell proliferation and apoptosis in HT29 cells revealed augmented phosphorylation of p-38 and Chk2. The p-38 pathway constitutes a critical regulator of apoptosis in tumor cells, involved in cascades that culminate in cell death and has been shown to be associated with extracellular stimuli, including chemotherapeutic agents [31, 32]. Phosphorylated Chk2 is a critical component of DNA damage response and plays a crucial role in cell cycle checkpoint activation, triggering proteins that regulate cell cycle arrest and apoptosis [33, 34], even sharing targets with p-38, such as Cdc25 family proteins [31, 34]. On the other hand, in HT29 cells co-cultured with the probiotic phosphorylation of Akt was markedly reduced. Akt is a serine/threonine kinase implicated in cell growth, proliferation, and survival. Phosphorylation of Akt activates it and overexpression of p-Akt is a common characteristic in various cancers and associated with a poor prognosis and worse overall survival [35, 36]. Another phosphorylation event that was found to be downregulated was that of HSP27. HSP27 is a potent anti-apoptotic mediator, able to bind and inhibit apoptosis effector proteins, such as caspase 3 and cytochrome c, while simultaneously binding and activating kinase Akt and stabilizing cytoskeletal elements. Moreover, the phosphorylated HSP27 has been shown to interact with intermediate proteins

that connect Fas (CD95) signaling to downstream kinases that facilitate cell death [37, 38].

Prompted by all of these observations, we decided to investigate the activity of the characteristic initiator caspases of both the extrinsic and intrinsic pathways of apoptosis [15]. Intriguingly, caspase 8 activation is evident well before caspase 9, by at least 12 h. Caspase 8, apart from directly cleaving and activating caspase 3, also cleaves the protein Bid, which then activates pro-apoptotic proteins [27], including Bax, facilitating MOMP and connecting extrinsic with intrinsic apoptosis [27, 28]. This sequential enhancement of caspase activity, in combination with the early upregulation of death receptors and the fact that various anti-apoptotic regulatory elements that protect from stress-induced cell death, such as catalase [39], HO-2 [40] and HSPs [38] do not appear to be downregulated from treatment with the probiotic is an indication that the pro-apoptotic activity of the microorganism can be mostly associated to death receptor signaling. Finally, in order to further corroborate that the apoptotic cascade is reaching its eventual conclusion, as we have previously shown [12], we evaluated the activation of effector caspase 3, the final stage of almost all initiating apoptosis modes [15, 17, 27], which we found to be evident in both cancer cell lines. We also noted decreased levels of claspin, a primarily checkpoint adaptor protein that has been shown to be overexpressed in cancer cells and even protect cancer cells through checkpoint-independent processes. In addition, claspin undergoes degradation by either caspases 3 and 7 or the proteasome during apoptosis, which eliminates Chk1 activation and halts the cell survival pathway mediated by Chk1 [41, 42]. More importantly, we detected cleavage of PARP1, a crucial nuclear regulator of cell homeostasis, including its ability to bind damaged DNA and facilitate recruitment of DNA damage repair proteins. PARP1 is a target of various cell death-inducing proteases, among them caspase 3, where cleavage of PARP1 produces characteristic fragments of 89 kDa and 24 kDa, with the larger fragment that contains the catalytic center released from the nucleus, while the smaller fragment irreversibly binds to DNA, acting as an inhibitor of both active PARP1 and enzymes that attempt to repair DNA damage [43, 44].

The prevalence of colorectal cancer, combined with the shortcomings of traditional therapeutic approaches, necessitates the investigation of alternative treatments. Various probiotic strains as well as metabolites or bioactive components thereof have been studied as potential anticancer compounds. Polysaccharide of *Lactobacillus casei* SB27 has been shown to reduce colon cancer cell proliferation and migration, increasing the activity of apoptotic caspases. These effects were mediated by upregulation of histidine triad nucleotide binding protein 2 (HINT2) and mitochondrial damage due to accumulation of calcium ions in them [45]. Similarly, Sun et al. [46] identified exopolysaccharides isolated from *Lactobacillus plantarum*-12 as more effective in inducing apoptosis among a panel of various lactobacilli strains, with the extract inhibiting the expression of proliferating cell nuclear antigen (PCNA) and increasing caspase activity and the Bax/Bcl-2 ratio, once again indicating activation of the mitochondrial apoptosis pathway. Apart from polysaccharides, intact bacteria [47], cell-free supernatants [48], peptidoglycans [49], and extracts from lactobacilli [50] have been shown to exert anti-proliferative effects and induce apoptosis on colon cancer cells.

One special case of bioactive compounds produced by lactic acid bacteria worth mentioning is the biosynthesis of selenium nanoparticles. Selenium is a vital element, integral to human health, with crucial involvement in immune system development as well as cancer prevention and treatment. Selenium nanoparticles and their unique properties hold potential as an alternative anticancer agent with applications in various fields and among the diverse synthesis methods of selenium nanoparticles, the green chemistry approach holds a distinctive position within nanotechnology [51]. Nanoparticles synthesized by *Lactobacillus casei* has been shown to impact the survival of colon cancer cells, inducing apoptosis and also inhibit their migration capacity [52]. In addition, our team has previously reported that nanoparticles synthesized by the strain ATCC 393 not only facilitate apoptotic death of colon cancer cells, but also possess immunomodulatory properties, mobilizing adaptive immune responses [24, 25].

Our next goal was to investigate the possibility that treatment of cancer cells with the probiotic could induce a special pattern of programmed cell death capable of eliciting adaptive immune responses, named immunogenic cell death. The immunogenicity in this case arises from the combination of tumor cell antigens and released DAMPs from dying cancer cells [20–22]. Our experiments unveiled a similar pattern of translocation of HMGB1 from the nucleus to the cytoplasm, exposure of calreticulin on the outer surface of the cytoplasmic membrane, and ATP release from the cells in both CT26 and HT29 cells incubated with *L. casei*. These events are well-studied and characterized markers of immunogenic cell death, giving rise to potent adjuvanticity to dying cancer cells.

Calreticulin, an endoplasmic reticulum chaperone in normal conditions, relocates to the cell membrane under immunogenic cell death [22, 26, 53], where it is recognized by the LDL-receptor-related protein 1 (LRP1 or CD91) of antigen-presenting cells, such as dendritic cells and promotes the engulfment of dying cells and their remains [26, 54]. Interestingly, its localization during immunogenic cell death is associated with the activation of caspase 8 and Bax oligomerization, but precedes the distinctive morphological attributes of apoptosis [55].

HMGB1 is a nuclear protein, partaking in the organization of DNA and transcription regulation [56]. Nevertheless, under the right conditions it exits the nucleus and in the cytosol acts as an inflammasome enabler, as well as a modulator of apoptosis and autophagy, and can even be secreted or passively released from dying cells and possess potent cytokine and chemokine activities [20, 56]. Extracellular HMGB1 is recognized by a variety of myeloid cell-expressed receptors, such as advanced glycosylation end-product-specific receptor (RAGE) and toll-like receptor 4 (TLR4); however, it appears that its interaction with TLR4 is the most crucial for the perception of immunogenicity [20, 57]. Intriguingly, identification of extracellular HMGB1 by dendritic cells (DC) induces DC-mediated immune responses that culminate in the maturation and expansion of tumor specific CD4 and CD8 T cells and enhanced antitumor activity [21, 58, 59].

ATP is a small metabolite used as an energy source in cell processes that in the concept of immunogenic cell death is released from cells and represents a potent chemo attractant and immunostimulatory signal [60, 61]. Extracellular ATP can bind with the purinergic receptor P2Y2 (P2RY2) on precursor myeloid cells acting as a homing signal [22, 62], or purinergic receptor P2X7 (P2RX7) inducing inflammasome activation and secretion of IL-1β and IL-18 [63, 64]. Interestingly, these functions are seemingly more interchangeable than initially believed [65], and both appear to be necessary in order for DC-mediated priming of tumor-specific adaptive immune responses and the recruitment of γδ T cells that secrete IL-17 and facilitate tumor infiltration of cytotoxic T cells [66].

Finally, type I IFN is another identified immunogenic cell death hallmark [20, 26]. Type I IFN production can be induced by binding of nucleic acids [67] through various receptors. In any case, the presence of type I IFN facilitates potent immunostimulatory cascades, mediated by immune cells [68–70], such as enhancement of cytotoxic activity of CD8 T cells and NK cells [71], cross-priming by DCs [72, 73] and macrophage-derived production of pro-inflammatory agents [74]. Type I IFN signaling appears to be a critical component of the immunogenicity arising following treatment with anthracyclines or radiation [67, 75].

In conclusion, the present study attempted to dive deeper in the anti-proliferative effect of *Lacticaseibacillus casei* ATCC 393 against colonic cancer cells CT26 and HT29 and investigate the possibility of the probiotic-inducing immunogenic cell death. To this end, we detected in both cell lines notable pro-apoptotic signaling and modulation of protein expression, highlighted by the up-regulation of death receptors that initiate the extrinsic apoptotic pathway. In agreement with this observation, caspase 8, the initiator caspase involved in this pathway appeared to be active in the early stages of the apoptotic cascade triggered by *L. casei*, followed by the activation of caspase 9 later on and ultimately and more importantly caspase 3, the principal executioner caspase that facilitates the destabilization of cellular integrity and eventual death. Next, we examined the release of DAMPs associated with immunogenic cell death and capable of promoting adaptive immune responses. Intriguingly, following treatment of both CT26 and HT29 cells with *L. casei*, we detected the exposure of the endoplasmatic reticulum chaperone calreticulin on the outer layer of the cell membrane, as well as the translocation of the protein HMGB1 from the nucleus to the cytoplasm and eventually outside the cell. In addition, the ATP content of both treated cancer cell lines was diminished and type I IFN expression was upregulated, at least in CT26 cells. Our results suggest that treatment with *L. casei* induced the apoptotic clearance of colon cancer cells, primarily through extrinsic death receptor signaling and also resulted in the release of well-studied DAMPs, associated with immunogenic cell death and the subsequent induction of adaptive immune responses. To our knowledge, this is one of very few instances of immunogenic cells death reported in response to probiotic treatment of cancer cells. Further studies are also warranted in order to assess the potential of *L. casei* induced cancer cell death to actually elicit adaptive immune responses and the maturation of immune cell populations capable of driving successful tumor cell extermination.

Supplementary Information The online version contains supplementary material available at https://doi.org/10.1007/s12602-024-10330-3.

Acknowledgements Part of the research project was supported by the Hellenic Foundation for Research and Innovation (H.F.R.I.) under the "1st Call for H.F.R.I. Research Projects to support Faculty members and Researchers and the procurement of high-cost research equipment" (Project Number: HFRI-FM17C3-2007).

Authors' Contributions G.A., V.G., K.F., A.M. and K.S. performed the experiments and did the analysis. G.A. prepared the figures. G.A. and K.C. conceptualised the study and wrote the manuscript. All authors reviewed the manuscript and approved it for publication.

Data Availability Data is provided within the manuscript.

Declarations

Competing Interests The authors declare no competing interests.

References

1. Gibson GR, Hutkins R, Sanders ME, Prescott SL, Reimer RA, Salminen SJ et al (2017) Expert consensus document: The International Scientific Association for Probiotics and Prebiotics (ISAPP) consensus statement on the definition and scope of prebiotics. Nat Rev Gastroenterol Hepatol 14(8):491–502. https://doi.org/10.1038/nrgastro.2017.75

2. Wang Y, Wu J, Lv M, Shao Z, Hungwe M, Wang J et al (2021) Metabolism characteristics of lactic acid bacteria and the expanding applications in food industry. Front Bioeng Biotechnol 9:612285
3. Kim K-T, Yang SJ, Paik H-D (2021) Probiotic properties of novel probiotic Levilactobacillus brevis KU15147 isolated from radish kimchi and its antioxidant and immune-enhancing activities. Food Sci Biotechnol 30(2):257–265
4. Kumar H, Bhardwaj K, Valko M, Alomar SY, Alwasel SH, Cruz-Martins N et al (2022) Antioxidative potential of Lactobacillus sp. in ameliorating D-galactose-induced aging. Appl Microbiol Biotechnol 106(13–16):4831–4843. https://doi.org/10.1007/s00253-022-12041-7
5. Lee J-E, Lee N-K, Paik H-D (2021) Antimicrobial and antibiofilm effects of probiotic Lactobacillus plantarum KU200656 isolated from kimchi. Food Sci Biotechnol 30(1):97–106
6. Kariyawasam KMGMM, Yang SJ, Lee N-K, Paik H-D (2020) Probiotic properties of Lactobacillus brevis KU200019 and synergistic activity with fructooligosaccharides in antagonistic activity against foodborne pathogens. Food Sci Anim Resour 40(2):297–310
7. Chen Y-H, Tsai W-H, Wu H-Y, Chen C-Y, Yeh W-L, Chen Y-H et al (2019) Probiotic Lactobacillus spp. act against Helicobacter pylori-induced inflammation. J Clin Med 8(1):90
8. Jung J-I, Kim YG, Kang C-H, Imm J-Y (2022) Effects of Lactobacillus curvatus MG5246 on inflammatory markers in Porphyromonas gingivalis lipopolysaccharide-sensitized human gingival fibroblasts and periodontitis rat model. Food Sci Biotechnol 31(1):111–120
9. Aindelis G, Tiptiri-Kourpeti A, Lampri E, Spyridopoulou K, Lamprianidou E, Kotsianidis I et al (2020) Immune responses raised in an experimental colon carcinoma model following oral administration of *Lactobacillus casei*. Cancers (Basel) 12(2):368
10. Foysal MJ, Fotedar R, Siddik MAB, Tay A (2020) Lactobacillus acidophilus and L. plantarum improve health status, modulate gut microbiota and innate immune response of marron (Cherax cainii). Sci Rep 10(1):5916. https://doi.org/10.1038/s41598-020-62655-y
11. Aindelis G, Chlichlia K (2020) Modulation of anti-tumour immune responses by probiotic bacteria. Vaccines 8(2):329
12. Tiptiri-Kourpeti A, Spyridopoulou K, Santarmaki V, Aindelis G, Tompoulidou E, Lamprianidou EE et al (2016) *Lactobacillus casei* exerts anti-proliferative effects accompanied by apoptotic cell death and up-regulation of TRAIL in colon carcinoma cells. PLoS ONE 11(2):1–20
13. Nowak A, Paliwoda A, Błasiak J (2019) Anti-proliferative, pro-apoptotic and anti-oxidative activity of Lactobacillus and Bifidobacterium strains: a review of mechanisms and therapeutic perspectives. Crit Rev Food Sci Nutr 59(21):3456–3467. https://doi.org/10.1080/10408398.2018.1494539
14. Chuah L-O, Foo HL, Loh TC, Mohammed Alitheen NB, Yeap SK, Abdul Mutalib NE et al (2019) Postbiotic metabolites produced by Lactobacillus plantarum strains exert selective cytotoxicity effects on cancer cells. BMC Complement Altern Med 19(1):114
15. Galluzzi L, Vitale I, Aaronson SA, Abrams JM, Adam D, Agostinis P et al (2018) Molecular mechanisms of cell death: recommendations of the Nomenclature Committee on Cell Death 2018. Cell Death Differ 25(3):486–541
16. Pentimalli F, Grelli S, Di Daniele N, Melino G, Amelio I (2019) Cell death pathologies: targeting death pathways and the immune system for cancer therapy. Genes Immun 20(7):539–554. https://doi.org/10.1038/s41435-018-0052-x
17. Pistritto G, Trisciuoglio D, Ceci C, Garufi A, D'Orazi G (2016) Apoptosis as anticancer mechanism: function and dysfunction of its modulators and targeted therapeutic strategies. Aging (Albany NY) 8(4):603–619
18. Dadsena S, King LE, García-Sáez AJ (2021) Apoptosis regulation at the mitochondria membrane level. Biochim Biophys acta Biomembr 1863(12):183716
19. Birmpilis AI, Paschalis A, Mourkakis A, Christodoulou P, Kostopoulos IV, Antimissari E et al (2022) Immunogenic cell death, DAMPs and prothymosin α as a putative anticancer immune response biomarker. Cells 11(9):1–21
20. Galluzzi L, Vitale I, Warren S, Adjemian S, Agostinis P, Martinez AB et al (2020) Consensus guidelines for the definition, detection and interpretation of immunogenic cell death. J Immunother Cancer 8(1):1–21
21. Galluzzi L, Humeau J, Buqué A, Zitvogel L, Kroemer G (2020) Immunostimulation with chemotherapy in the era of immune checkpoint inhibitors. Nat Rev Clin Oncol 17(12):725–741
22. Kroemer G, Galassi C, Zitvogel L, Galluzzi L (2022) Immunogenic cell stress and death. Nat Immunol 23(4):487–500. https://doi.org/10.1038/s41590-022-01132-2
23. Vichai V, Kirtikara K (2006) Sulforhodamine B colorimetric assay for cytotoxicity screening. Nat Protoc 1(3):1112–1116
24. Spyridopoulou K, Aindelis G, Pappa A, Chlichlia K (2021) Anticancer activity of biogenic selenium nanoparticles: apoptotic and immunogenic cell death markers in colon cancer cells. Cancers (Basel) 13(21):5335
25. Spyridopoulou K, Tryfonopoulou E, Aindelis G, Ypsilantis P, Sarafidis C, Kalogirou O et al (2021) Biogenic selenium nanoparticles produced by: Lactobacillus casei ATCC 393 inhibit colon cancer cell growth in vitro and in vivo. Nanoscale Adv 3(9):2516–2528
26. Fucikova J, Kepp O, Kasikova L, Petroni G, Yamazaki T, Liu P, et al (2020) Detection of immunogenic cell death and its relevance for cancer therapy. Cell Death Dis 11(11). https://doi.org/10.1038/s41419-020-03221-2
27. Tummers B, Green DR (2017) Caspase-8: regulating life and death. Immunol Rev 277(1):76–89
28. Kalkavan H, Green DR (2018) MOMP, cell suicide as a BCL-2 family business. Cell Death Differ 25(1):46–55. https://doi.org/10.1038/cdd.2017.179
29. Warrier NM, Agarwal P, Kumar P (2020) Emerging importance of survivin in stem cells and cancer: the development of new cancer therapeutics. Stem Cell Rev Reports 16(5):828–852
30. Guo W, Ma X, Fu Y, Liu C, Liu Q, Hu F et al (2021) Discovering and characterizing of survivin dominant negative mutants with stronger pro-apoptotic activity on cancer cells and CSCs. Front Oncol 11(March):1–13
31. Canovas B, Nebreda AR (2021) Diversity and versatility of p38 kinase signalling in health and disease. Nat Rev Mol Cell Biol 22(5):346–366. https://doi.org/10.1038/s41580-020-00322-w
32. Chen L, Jiang K, Chen H, Tang Y, Zhou X, Tan Y et al (2019) Deguelin induces apoptosis in colorectal cancer cells by activating the p38 MAPK pathway. Cancer Manag Res 11:95–105
33. Zannini L, Delia D, Buscemi G (2014) CHK2 kinase in the DNA damage response and beyond. J Mol Cell Biol 6(6):442–457
34. Zhang M, Qu J, Gao Z, Qi Q, Yin H, Zhu L et al (2021) Timosaponin AIII induces G2/M arrest and apoptosis in breast cancer by activating the ATM/Chk2 and p38 MAPK signaling pathways. Front Pharmacol 11(January):1–15
35. He Y, Sun MM, Zhang GG, Yang J, Chen KS, Xu WW et al (2021) Targeting PI3K/Akt signal transduction for cancer therapy. Signal Transduct Target Ther 6(1):425
36. Yao Z, Gao G, Yang J, Long Y, Wang Z, Hu W et al (2020) Prognostic role of the activated p-AKT molecule in various hematologic malignancies and solid tumors: a meta-analysis. Front Oncol 10(December):1–10

37. Katsogiannou M, Andrieu C, Rocchi P (2014) Heat shock protein 27 phosphorylation state is associated with cancer progression. Front Genet 5(SEP):1–5
38. Wang X, Chen M, Zhou J, Zhang X (2014) HSP27, 70 and 90, anti-apoptotic proteins, in clinical cancer therapy (review). Int J Oncol 45(1):18–30
39. Glorieux C, Calderon PB (2017) Catalase, a remarkable enzyme: targeting the oldest antioxidant enzyme to find a new cancer treatment approach. Biol Chem 398(10):1095–1108
40. Muñoz-Sánchez J, Chánez-Cárdenas ME (2014) A review on hemeoxygenase-2: focus on cellular protection and oxygen response. Oxid Med Cell Longev 2014:25–28
41. Semple JI, Smits VAJ, Fernaud JR, Mamely I, Freire R (2007) Cleavage and degradation of Claspin during apoptosis by caspases and the proteasome. Cell Death Differ 14(8):1433–1442
42. Bianco JN, Bergoglio V, Lin YL, Pillaire MJ, Schmitz AL, Gilhodes J, et al (2019) Overexpression of Claspin and Timeless protects cancer cells from replication stress in a checkpoint-independent manner. Nat Commun 10(1). https://doi.org/10.1038/s41467-019-08886-8
43. Chaitanya GV, Alexander JS, Babu PP (2010) PARP-1 cleavage fragments: Signatures of cell-death proteases in neurodegeneration. Cell Commun Signal 8:31. https://doi.org/10.1186/1478-811X-8-31
44. Mashimo M, Onishi M, Uno A, Tanimichi A, Nobeyama A, Mori M et al (2021) The 89-kDa PARP1 cleavage fragment serves as a cytoplasmic PAR carrier to induce AIF-mediated apoptosis. J Biol Chem 296:100046. https://doi.org/10.1074/jbc.RA120.014479
45. Di W, Li X, Yang Q (2023) Polysaccharide of Lactobacillus casei SB27 reduced colon cancer cell prognosis through mitochondrial damage by upregulation of HINT2. Asia Pac J Clin Oncol 19(5):e248–e257
46. Sun M, Liu W, Song Y, Tuo Y, Mu G, Ma F (2021) The effects of Lactobacillus plantarum-12 crude exopolysaccharides on the cell proliferation and apoptosis of human colon cancer (HT-29) cells. Probiotics Antimicrob Proteins 13(2):413–421
47. Yue Y, Wang S, Shi J, Xie Q, Li N, Guan J et al (2022) Effects of Lactobacillus acidophilus KLDS1.0901 on proliferation and apoptosis of colon cancer cells. Front Microbiol 12(February):1–15
48. Salemi R, Vivarelli S, Ricci D, Scillato M, Santagati M, Gattuso G et al (2023) Lactobacillus rhamnosus GG cell-free supernatant as a novel anti-cancer adjuvant. J Transl Med 21(1):1–17. https://doi.org/10.1186/s12967-023-04036-3
49. Fuochi V, Spampinato M, Distefano A, Palmigiano A, Garozzo D, Zagni C et al (2023) Soluble peptidoglycan fragments produced by Limosilactobacillus fermentum with antiproliferative activity are suitable for potential therapeutic development: a preliminary report. Front Mol Biosci 10(February):1–12
50. Amin M, Navidifar T, Saeb S, Barzegari E, Jamalan M (2023) Tumor-targeted induction of intrinsic apoptosis in colon cancer cells by Lactobacillus plantarum and Lactobacillus rhamnosus strains. Mol Biol Rep 50(6):5345–5354
51. Zhang T, Qi M, Wu Q, Xiang P, Tang D, Li Q (2023) Recent research progress on the synthesis and biological effects of selenium nanoparticles. Front Nutr 10(May):1–12
52. Haji Mehdi Nouri Z, Tafvizi F, Amini K, Khandandezfully N, Kheirkhah B (2024) Enhanced induction of apoptosis and cell cycle arrest in MCF-7 breast cancer and HT-29 colon cancer cell lines via low-dose biosynthesis of selenium nanoparticles utilizing Lactobacillus casei. Biol Trace Elem Res 202(3):1288–304. https://doi.org/10.1007/s12011-023-03738-5
53. Schcolnik A, Bernardo C, Mandy O, Mayra J, Rivera C, Flisser A (2019) Calreticulin in phagocytosis and cancer : opposite roles in immune response outcomes. Apoptosis 24(3):245–55. https://doi.org/10.1007/s10495-019-01532-0
54. Garg AD, Krysko DV, Verfaillie T, Kaczmarek A, Ferreira GB, Marysael T et al (2012) A novel pathway combining calreticulin exposure and ATP secretion in immunogenic cancer cell death. EMBO J 31(5):1062–79. https://doi.org/10.1038/emboj.2011.497
55. Panaretakis T, Brockmeier U, Bjorklund A, Chapman DC, Durchschlag M, Joza N et al (2009) Mechanisms of pre-apoptotic calreticulin exposure in immunogenic cell death. EMBO J 28(5):578–90
56. Yang H, Wang H, Chavan SS, Andersson U (2015) High mobility group box protein 1 (HMGB1): the prototypical endogenous danger molecule. Mol Med 21:S6-12
57. Yang H, Hreggvidsdottir HS, Palmblad K, Wang H, Ochani M, Li J et al (2010) A critical cysteine is required for HMGB1 binding to toll-like receptor 4 and activation of macrophage cytokine release. Proc Natl Acad Sci U S A 107(26):11942–11947
58. Gao Q, Li F, Wang S, Shen Z, Cheng S, Ping Y et al (2019) A cycle involving HMGB1, IFN-γ and dendritic cells plays a putative role in anti-tumor immunity. Cell Immunol 343(August):1. https://doi.org/10.1016/j.cellimm.2018.08.011
59. Gebremeskel S, Johnston B (2015) Concepts and mechanisms underlying chemotherapy induced immunogenic cell death: Impact on clinical studies and considerations for combined therapies. Oncotarget 6(39):41600–41619
60. Martins I, Wang Y, Michaud M, Ma Y, Sukkurwala AQ, Shen S et al (2014) Molecular mechanisms of ATP secretion during immunogenic cell death. Cell Death Differ 21(1):79–91
61. Anderson CM, Macleod KF (2019)Autophagy and cancer cell metabolism [Internet]. 1st ed. Vol. 347, Cellular nutrient utilization and cancer. Elsevier Inc. pp 145–190. https://doi.org/10.1016/bs.ircmb.2019.06.002
62. Elliott MR, Chekeni FB, Trampont PC, Lazarowski ER, Kadl A, Walk SF et al (2009) Nucleotides released by apoptotic cells act as a find-me signal to promote phagocytic clearance. Nature 461(7261):282–6. https://doi.org/10.1038/nature08296
63. Ghiringhelli F, Apetoh L, Tesniere A, Aymeric L, Ma Y, Ortiz C et al (2009) Activation of the NLRP3 inflammasome in dendritic cells induces IL-1β–dependent adaptive immunity against tumors. Nat Med 15(10):1170–8. https://doi.org/10.1038/nm.2028
64. Swanson KV, Deng M, Ting JP-Y (2019) The NLRP3 inflammasome: molecular activation and regulation to therapeutics. Nat Rev Immunol 19(8):477–89. https://doi.org/10.1038/s41577-019-0165-0
65. Sáez PJ, Vargas P, Shoji KF, Harcha PA, Lennon-Duménil A-M, Sáez JC (2017) ATP promotes the fast migration of dendritic cells through the activity of pannexin 1 channels and P2X7 receptors. Sci Signal 10(506):eaah7107. https://doi.org/10.1126/scisignal.aah7107
66. Kepp O, Bezu L, Yamazaki T, Di Virgilio F, Smyth MJ, Kroemer G et al (2021) ATP and cancer immunosurveillance. EMBO J 40(13):e108130
67. Sistigu A, Yamazaki T, Vacchelli E, Chaba K, Enot DP, Adam J et al (2014) Cancer cell–autonomous contribution of type I interferon signaling to the efficacy of chemotherapy. Nat Med 20(11):1301–9. https://doi.org/10.1038/nm.3708
68. Hopfner KP, Hornung V (2020) Molecular mechanisms and cellular functions of cGAS–STING signalling. Nat Rev Mol Cell Biol 21(9):501–21. https://doi.org/10.1038/s41580-020-0244-x
69. McLaughlin M, Patin EC, Pedersen M, Wilkins A, Dillon MT, Melcher AA et al (2020) Inflammatory microenvironment remodelling by tumour cells after radiotherapy. Nat Rev Cancer 20(4):203–17. https://doi.org/10.1038/s41568-020-0246-1

70. Motwani M, Pesiridis S, Fitzgerald KA (2019) DNA sensing by the cGAS–STING pathway in health and disease. Nat Rev Genet 20(11):657–74. https://doi.org/10.1038/s41576-019-0151-1
71. Oh JH, Kim MJ, Choi SJ, Ban YH, Lee HK, Shin EC et al (2019) Sustained type I interferon reinforces NK cell–mediated cancer immunosurveillance during chronic virus infection. Cancer Immunol Res 7(4):584–599
72. Takeda Y, Azuma M, Funami K, Shime H, Matsumoto M, Seya T (2018) Type I interferon-independent dendritic cell priming and antitumor T cell activation induced by a Mycoplasma fermentans lipopeptide. Front Immunol 9(MAR):1–11
73. Bek S, Stritzke F, Wintges A, Nedelko T, Böhmer DFR, Fischer JC et al (2019) Targeting intrinsic RIG-I signaling turns melanoma cells into type I interferon-releasing cellular antitumor vaccines. Oncoimmunology 8(4):1–9. https://doi.org/10.1080/2162402X.2019.1570779
74. Müller E, Christopoulos PF, Halder S, Lunde A, Beraki K, Speth M et al (2017) Toll-like receptor ligands and interferon-γ synergize for induction of antitumor M1 macrophages. Front Immunol 8(OCT):1383
75. Vanpouille-Box C, Alard A, Aryankalayil MJ, Sarfraz Y, Diamond JM, Schneider RJ et al (2017) DNA exonuclease Trex1 regulates radiotherapy-induced tumour immunogenicity. Nat Commun 8:15618. https://doi.org/10.1038/ncomms15618